Turbulence-airfoil interaction noise reduction using wavy leading edge: an experimental and numerical study

Cyril Polacsek, Gabriel Reboul, Vincent Clair, Thomas Le Garrec, Guillaume Dufour, Hugues Deniau

18TH INTERNATIONAL CONGRESS ON SOUND & VIBRATION
ICSV18
RIO DE JANEIRO
BRAZIL
10–14 JULY 2011

TURBULENCE-AIRFOIL INTERACTION NOISE REDUCTION USING WAVY LEADING EDGE: AN EXPERIMENTAL AND NUMERICAL STUDY

Cyril Polacsek, Gabriel Reboul, Vincent Clair, Thomas Le Garrec

Office National d'Etudes et de Recherches Aérospatiales, Department of Numerical Simulations and Aeroacoustics, 92322 Châtillon Cedex, France
e-mail: cyril.polacsek@onera.fr

Guillaume Dufour, Hugues Deniau

Centre Européen de Recherche et de Formation Avancée en Calcul Scientifique CFD Team, 31057 Toulouse Cedex 01, France

Passive treatments aiming at reducing turbofan broadband noise have been recently studied in the framework of European Project FLOCON. A concept based on a sinusoidal variation of the leading edge of a single airfoil aiming at reducing interaction noise has been investigated by ONERA. Turbulence-airfoil interaction mechanism is achieved using a turbulence grid located upstream of a NACA airfoil tested in ISVR anechoic open wind tunnel. High noise reductions are obtained (3-4 dB) for all studied flow speeds. Moreover, aerodynamic performances are shown to be slightly increased by the treatment that tends to reduce the drag without modify the mean loading. Experimental work is supplemented by numerical simulations using Large Eddy Simulations (LES) and direct Euler approaches to predict the acoustic response of the wing. LES is chained to a FWH (Ffowcs-Williams and Hawkings) integral to assess the radiated field. Isentropic turbulence is synthetically injected by means of a suited inflow boundary condition. Present computations are focused on the reference case (without treatment). Numerical predictions are compared to the experiment, and to analytical solutions issued from Amiet theory.

1. Introduction

Turbulent wakes generated by turbofan blades and interacting with the OGV are known to be mainly contributing to broadband noise emission of aeroengines at approach conditions. Passive treatments aiming at reducing fan broadband noise have been recently studied in the framework of European Project FLOCON[1,2]. A concept based on a tri-dimensional sinusoidal modification of the LE (leading edge) of a single airfoil has been investigated by ONERA. Turbulence-airfoil interaction mechanism is achieved using turbulence grids located upstream of a NACA 651210 airfoil in the ISVR anechoic open wind tunnel[3]. Three airfoil sets with different values for wavelength and wave amplitude have been tested and compared to the reference wing response. A circular microphone antenna located at about three spans from the airfoil provides acoustic spectra and OASPL

(Overall Sound Pressure Level) directivity. High noise reductions are measured (up to 6 dB/Hz) for a wide frequency range, leading to at least 3 dB attenuation of acoustic power. Moreover, aerodynamic performances are shown to be slightly increased by the treatment that tends to reduce the turbulent wake intensity beyond the TE (trailing edge), the (spanwise averaged) static pressure distribution being roughly unchanged. Experimental work is supplemented by CAA (Computational Aero-Acoustics) aiming to simulate the aerodynamic and acoustic responses. Present computations are focused on the reference case (no treatment). First predictions based on analytical Amiet formulation[4] are found to be close to the measurements, but extension of the theory to varying edges seems too complex. In order to try to take into account true airfoil geometry and realistic mean flow, numerical simulations issued from 3D LES[5] and 2D non-linearized Euler computations are proposed. In both cases, HIT (homogeneous isentropic turbulence) is synthetically injected by means of divergence-free velocity disturbance field distributed over Fourier-modes with random phases. CAA is coupled to usual integral methods to assess the acoustic far-field. Numerical predictions (spectra and directivities) are compared to the experiment, and capability of each method is discussed.

2. Wavy leading edge concept description

Wavy edge treatment has been recently studied by Hansen et al.[5] for aerodynamic performance purpose, following previous investigations on aerodynamic effects of whale flipper leading-edge rounded protuberances (so-called tubercles)[6]. It was shown that tubercles act as vortex generators which could increase the lift and delay the stall.

Wavy-edge concept is illustrated in Fig. 1, showing a 3D CAD view with two main adjustment parameters (wavelength, λ and amplitude, A) and a picture of one of the manufactured ONERA wings. The present study is devoted to acoustic performances with respect to turbulence-airfoil interaction (broadband) noise reduction, assuming that acoustic sources are located in the leading edge region. Sinusoidal variations of the chord length and lean angle are expected to introduce some spanwise correlation loss and to modify the response to the impinging gusts (turning parallel cut-on modes to oblique cut-off modes).

Three sets of wing have been manufactured and tested :

- λ = 6 mm and A = 10 mm (referred as 1S)
- λ = 10 mm and A = 10 mm (referred as 2S)
- λ = 10 mm and A = 15 mm (referred as 3S)

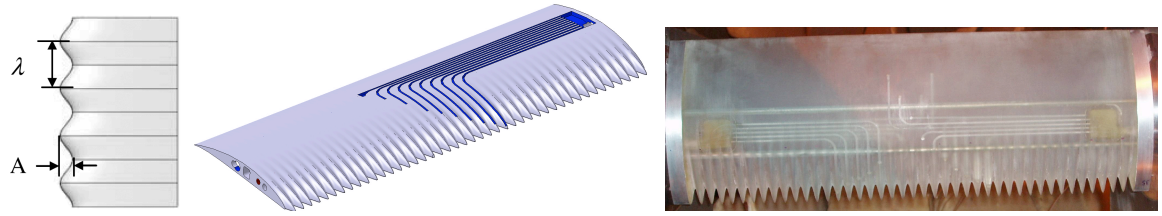

Figure 1. FLOCON wing design: CAD drawing (left) and manufactured wing (right)

3. Experimental set-up and acoustic performances

ONERA wings have been tested in the ISVR anechoic wind tunnel[2,3] and compared to the baseline case at several flow speeds (U_0 = 20, 40, 60 m/s) and for different angle of attack values (α= 0°, 5°, 10°, 15°). Experimental set-up is presented in Fig. 2, showing the circular antenna (located at 1.2 m from the airfoil) used to get the far-field PSD (Power Spectrum Density) and directivities. A square-bars turbulence grid located inside the nozzle

near the outlet allows to provide HIT characteristics (validated by comparison to usual Von-Karman spectrum) upstream of the airfoil, with a turbulence intensity, T_I = 2.5 %, and an integral length scale, Λ = 6 mm. Hence, interaction noise (measured with the grid) is found to be largely dominant compared to the airfoil self-noise, as shown in Fig. 3, for two flow speed values. PSD measured at 90° microphone for the three treatments are compared to the baseline in Fig. 4 (α = 0°), showing high noise reduction for a wide frequency range, more particularly at low speed. Best performances are obtained with treatment 3S. Fig. 4 summarizes the noise level reductions obtained with treatment 3S, by integrating the spectra in the range [300 Hz - 20 kHz]. It shows that good performances are reached for all angle of attack values up to α = 15°. Fig. 6 (left), proposes a PSD comparison between wing 3S and baseline (0S), highlighting large noise reductions in the mid-frequency range (about 6 dB at 3 kHz). OASPL directivity related to microphone antenna and calculated by integrating the spectra from 1 kHz is shown in Fig. 6 (right). Acoustic performances appear to be slightly reduced in the front arc region (-3 dB deviation) compared to the rear one (-5 dB deviation).

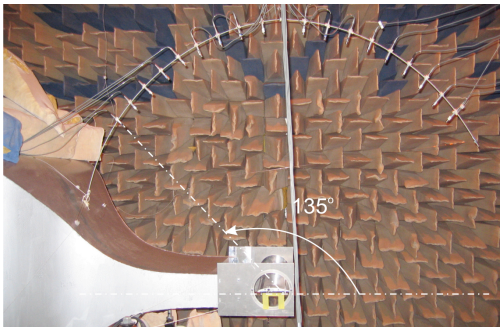

Figure 2. Experimental set-up in ISVR rig

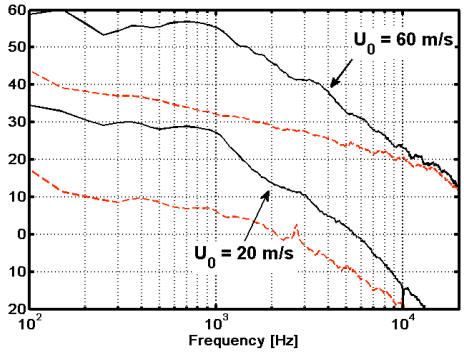

Figure 3. Interaction (black) and self (red) noise spectra

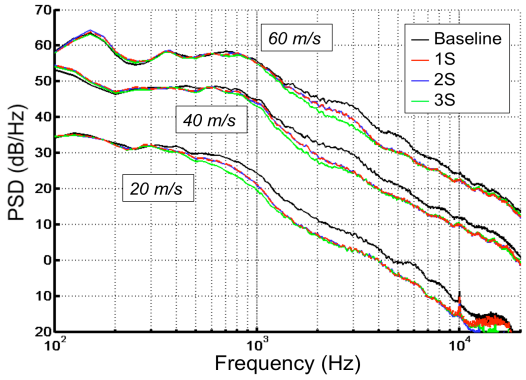

Figure 4. Baseline and ONERA wing spectra (90°)

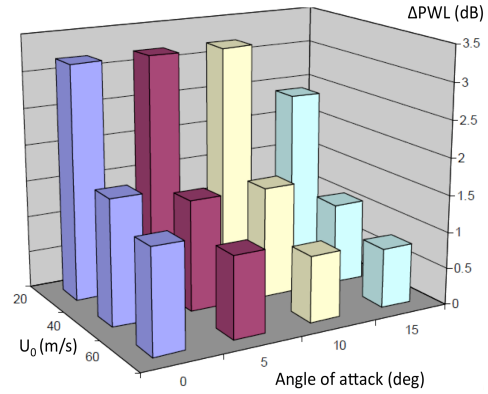

Figure 5. PWL reductions (dB) using S3 wing

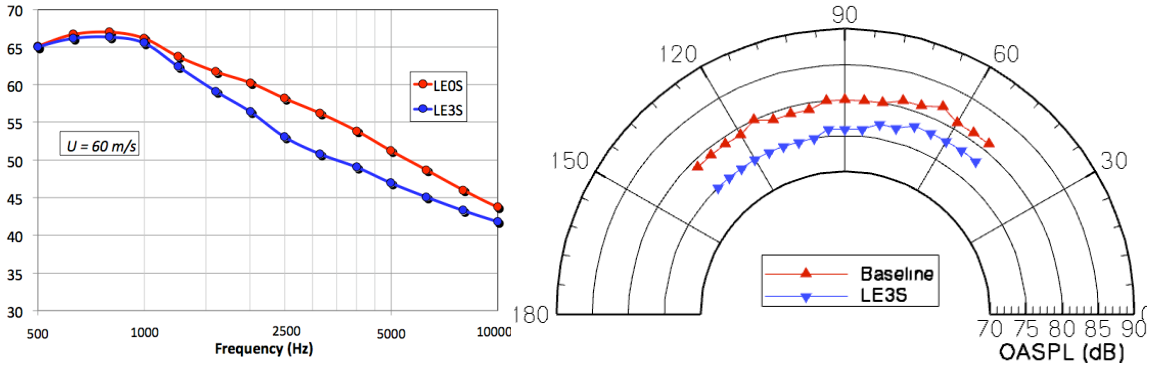

Figure 6. Baseline-3S PWL (dB) comparisons (left) and OASPL directivities (right)

4. Analytical and numerical predictions

4.1 Integral formulations and Amiet-based predictions

Following Amiet theory[4], the problem of turbulence-airfoil interaction can be modelized as a summation of harmonic gusts impinging a flat plate as sketched in Figure 1. The gusts are time and space Fourier-modes in the chordwise and spanwise directions. K_ζ and K_ξ are the aerodynamic wave numbers in the local coordinate system (ζ,η,ξ).

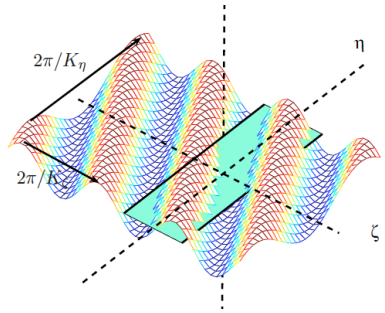

Figure 7. Sketch of gust-airfoil problem

The aerodynamic response of the airfoil, $g\left(\zeta,K_\varsigma,K_\xi\right)$, is calculated by solving a potential equation satisfying the convected wave equation. The wall-pressure jump, Δp, then writes:

$$\Delta p(\zeta,\eta,t)=2\pi\rho_0 U_c\int_{-\infty}^{+\infty}\int_{-\infty}^{+\infty}\hat{\hat{u}}_\xi\left(K_\varsigma,K_\xi\right)g\left(\zeta,K_\varsigma,K_\xi\right)e^{i\left(K_\zeta U_\varsigma t-K_\eta\eta\right)}dK_\zeta dK_\eta \qquad (1)$$

$\hat{\hat{u}}_\xi$ denotes the double space-Fourier transformation of incoming velocity fluctuation normal to the plate, and U_c is the chordwise velocity (taken equal to the convection velocity) related to the convection wave number using Taylor assumption (frozen turbulence): $K_\varsigma=K_c=\dfrac{\omega}{U_c}$. The radiated acoustic field is obtained by using Curle's formulation:

$$\hat{p}\left(\vec{X},\omega\right)=\int_S\hat{p}\left(\vec{Y},\omega\right)n_i\frac{\partial G_\omega\left(\vec{X},\vec{Y}\right)}{\partial y_i}dS \qquad (2)$$

where ^ denotes the time-Fourier transformation, $\vec{X}$ and $\vec{Y}$ are respectively the observer and source coordinates, and G_ω denotes the free-space time-Fourier transformed Green's function. The PSD of acoustic pressure, $S_{pp}\left(\vec{X},\omega\right)$, is estimated by injecting Eq. (1) in Eq. (2) and by performing the integral of the cross-conjugate product over spatial directions and spanwise wave-number. Far-field assumption (KR >>1) allows to make some great mathematical simplifications so that a rather concise expression can be obtained:

$$S_{pp}\left(\vec{X},\omega\right)=\left(\frac{kz\rho_0 b}{S_0^2}\right)^2 U_c d\pi\int_{-\infty}^{+\infty}\left|\frac{\sin^2\left(d\left(\dfrac{ky}{S_0}-K_\eta\right)\right)}{\pi d\left(\dfrac{ky}{S_0}-K_\eta\right)^2}\right|\left|\mathcal{L}\left(x,K_c,K_\eta\right)\right|^2\phi_{\xi\xi}\left(K_c,K_\eta\right)dK_\eta \qquad (3)$$

$\mathcal{L}$ is the aeroacoustic transfer function given by Amiet. The PSD of normal velocity fluctuation, $\phi_{\xi\xi}\left(K_c,K_\eta\right)$, can be estimated by means of a 2D Von-Karman turbulence energy spectrum model fitted by experimental input data (Λ and T_I). Predicted PSD at 90° and OASPL directivities are compared to the ISVR measurements in Figs 8 and 9, respectively.

A fairly good agreement is obtained, particularly for the lowest speed case. An under-estimation of the level attenuation slope can be noticed at higher speeds. This confirms that Amiet model is able to assess THI-airfoil noise, but extension of this theory to account for leading-edge treatment seems not feasible. This is the reason why numerical approach has been proposed and discussed in the next section.

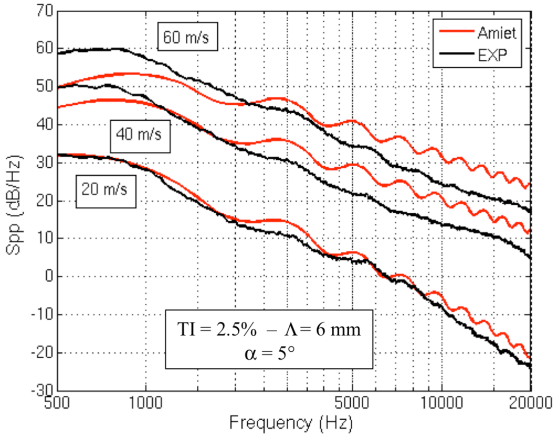

Figure 8. Predicted and measured PSD at 90°

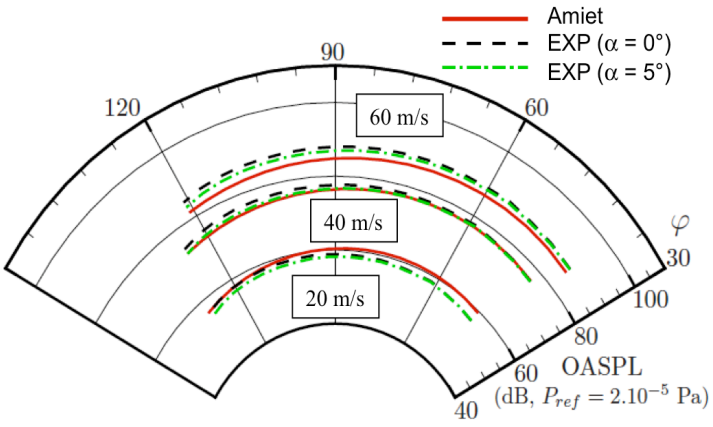

Figure 9. Predicted and measured OASPL directivities

4.2 Direct 2D Euler computations

In order to simulate the leading edge treatment effects on acoustics, a numerical methodology using ONERA code *sAbrinA*[8,9] has been investigated. The code solves the non-linear Euler disturbances in the time domain using a high-order DRP scheme. First computations are focused on the baseline case so that 2D simulations can be considered. Incoming turbulent flow is generated by means of harmonic velocity perturbations (following Amiet formalism) using a synthetic turbulence model[10,11], and injected through a suited inflow boundary condition[12]. As done in [10], only parallel gusts (K_ζ in Fig. 7) are imposed, with amplitudes adjusted using 1D Von-Karman energy spectrum as discussed in [11]. The turbulent transverse velocity fluctuation u_y (ξ direction in Fig. 7) then writes:

$$u_y(x,t) = \sum_{n=1}^{N_{\max}} \sqrt{\phi_{\xi\xi}(k_{c,n})\Delta k_c}\cos\left[k_{c,n}(x - U_c t) + \varphi_n\right],\ \varphi_n = random\{0,2\pi\} \qquad (4)$$

Realistic mean flow (U_c = 60 m/s) from nozzle exit is issued form a 2D RANS computation performed using ONERA code *elsA* (see [5] and next section). Iso-contour snapshot of turbulent velocity fluctuations impinging the airfoil is shown in Fig. 10 (left) and acoustic response in terms of pressure iso-contour snapshot is shown in Fig. 10 (right). Expected dipolar behavior is correctly assessed by the 2D simulation. Vortical waves convected along airfoil pressure side and beyond the trailing edge are clearly visible too.

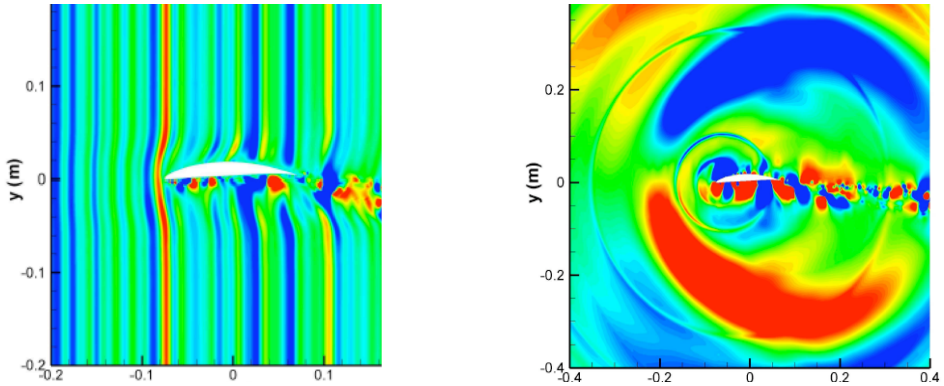

Figure 10. Synthetic turbulent velocity field (left) and direct acoustic pressure radiation (right)

Computed PSD at 90° for an observer at 0.35 m from the centre of the airfoil is presented in Fig. 11 (left, blue curve) and compared to the same simulation assuming a fully uniform flow (green curve with dots), and to the analytical solution issued from Amiet theory (dotted line). The agreement between CAA (uniform flow) and Amiet predictions is quite good, whereas a higher attenuation slope can be noticed for the CAA solution with a RANS mean flow. This could explain the slope deviation observed in Fig. 8 (left) and discussed in section 4.1. Similar comparisons on OASPL directivities are proposed in Fig. 11 (right), showing that the three predictions are almost identical in the front arc and that differences with Amiet solution are more marked in the upside rear arc. Upside/downside dissymmetry due to the fact that the airfoil is not symmetrical (whereas it is assumed to be in Amiet theory) is clearly highlighted by the CAA.

In order to compare the 2D simulations with the ISVR measurements, a simple correction proposed by Ewert[13] is applied to the PSD. It writes:

$$S_{pp}^{3D} = S_{pp}^{2D} \times \frac{k\ell_y(\omega)L}{2\pi R_{obs}} \tag{5}$$

ℓ_y is the spanwise correlation length (scaled from L and Von-Karman model), and L is the airfoil span. This correction was checked and found to be very accurate when applied to Amiet 2D and 3D direct solutions. PSD so obtained at 1.2 m (90°) microphone is compared to the measurements in Fig. 12. Smoothed CAA curve (pink curve) is found to be very close to the experiment (red curve) in the range [500 Hz – 5 kHz].

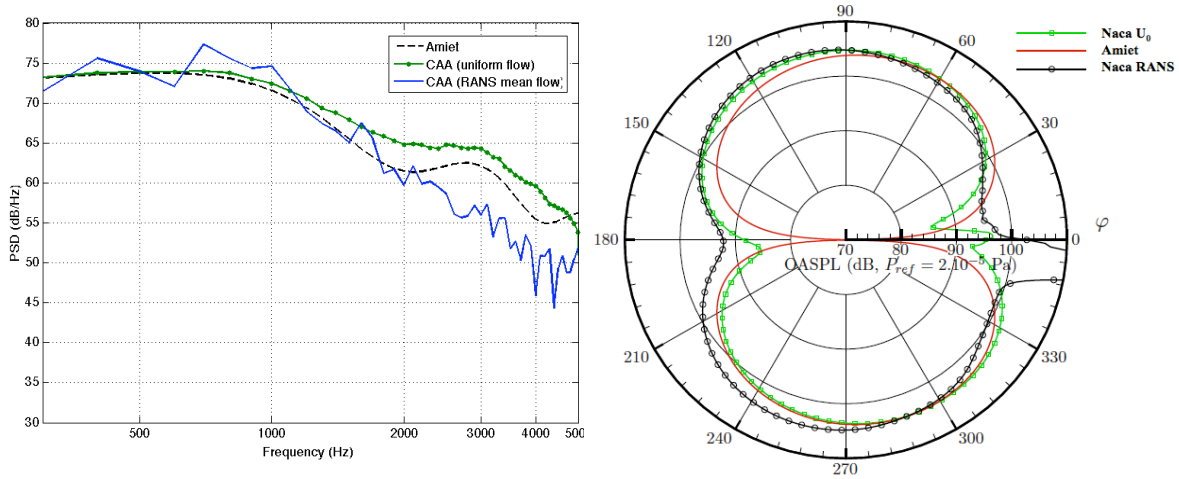

Figure 11. Predicted 2D spectra (dB/Hz) and OASPL (dB) directivities

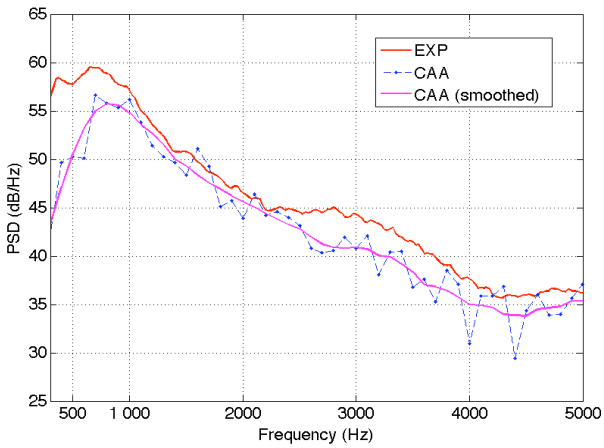

Figure 12. Predicted and measured 3D spectra (dB/Hz)

4.3 LES-FWH computations

A second numerical approach consisting in chaining a RANS-LES simulation to a FWH integral (Eq. (2)) has been investigated too, on baseline case. Hybrid RANS-LES strategy using ONERA code *elsA* is detailed in [5]. CFD domain with iso-contour Mach map computed by 2D RANS is shown in Fig. 13. The nozzle exit is included in the RANS domain to take into account for a realistic jet mean flow (60 m/s case) leading to a deviation of the downstream flow. Turbulent inflow is injected using the same synthetic turbulence model as in section 4.2. Quasi-3D computations are performed by extruding the 2D mesh over 100 planes, covering 60 mm (4 chords) in the spanwise direction. Full span contribution to acoustics is estimated applying usual basic correction as done by Kato[14]. To prevent from the occurrence of a re-circulation bubble[5] on the leading edge suction side observed at angles of attack $\alpha = 0°$ and 5°, simulations are performed at $\alpha = 10°$.

Iso-contour map of RMS wall-pressure field is shown in Fig. 14. It reveals expected sources in the LE region (interaction noise), but also high spot at the TE (self-noise), more particularly on the pressure side. These sources can be attributed to some interactions with convected vortexes (numerical artifacts ?) not present in the Euler simulations, and probably negligible in the experiment (see spectra comparison in Fig. 3). Consequently, PSD calculated by integrating the turbulent pressure fluctuations over the entire airfoil surface (LES domain) lead to an over-estimation of the levels. This is illustrated in Fig. 15 (left) comparing two LES-FWH predictions, using full integration (in red) and partial LE region integration (in blue), with the experiment (pink symbols). A better agreement is obtained when the TE contribution is discarded. However, an unexplained shift in frequency can be observed (peak around 1500 Hz instead of 750 Hz). Same comparisons on OASPL directivities are proposed in Fig. 15 (right). A good agreement is obtained when limiting the integration to the LE region (since the PSD levels are only shifted in frequency in that case).

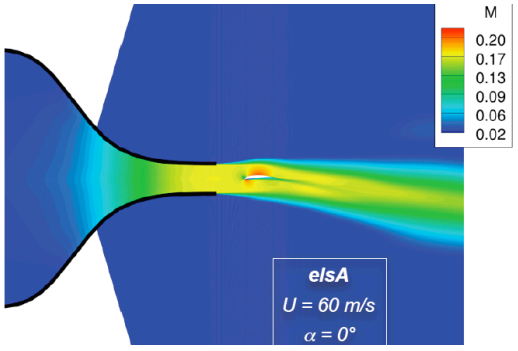

Figure 13. CFD domain and RANS mean flow

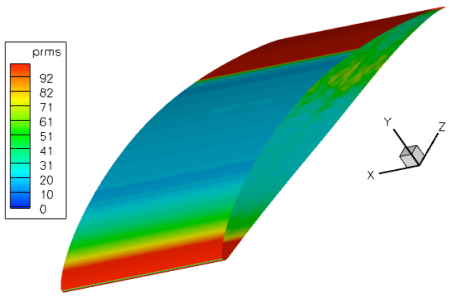

Figure 14. RMS wall-pressure issued from LES

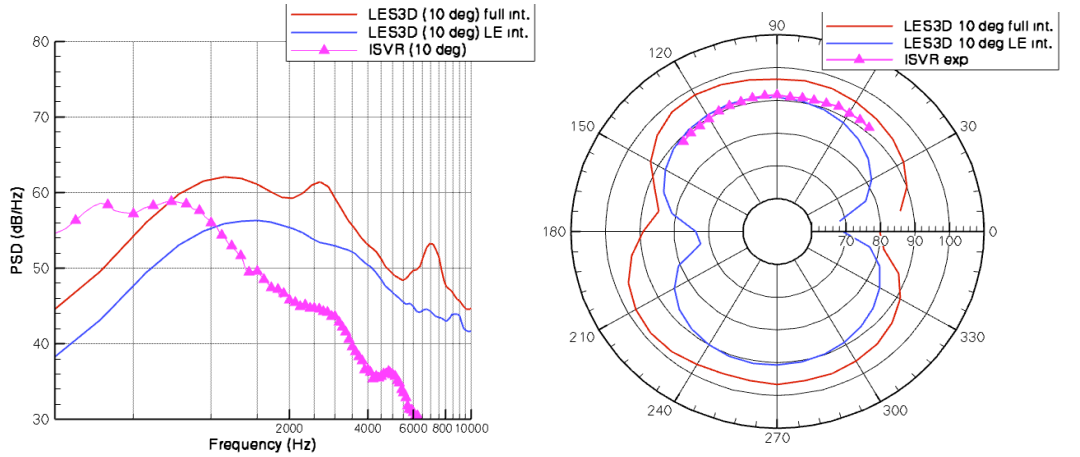

Figure 15. Predictions vs. measurement (pink symbols): PSD at 90° (left) and OASPL directivities (right) calculated using full (red) or partial (blue) FWH integration

5. Conclusions

A wavy leading edge treatment consisting in tridimensional sinusoidal serrations devoted to turbulence-airfoil interaction noise reduction has been applied to an isolated NACA airfoil impacted by a turbulent flow. Experimental data issued from wind tunnel tests have shown significant broadband noise reductions for a wide frequency range, and for almost all configurations. Aerodynamic performances suggested by recent studies have been partly confirmed too. This makes this concept very attractive for quieter industrial turbofans. Different methodologies aiming at simulating the acoustic efficiency of the treatment have been presented and discussed. First predictions are performed on the baseline case (no treatment). Analytical calculations based on Amiet theory are found to be quite reliable to estimate the interaction noise emitted by a standard airfoil, but extension of the theory to leading edge serrations seems not feasible. Thus, two numerical strategies have been proposed: A direct method based on Euler computation (neglecting viscosity effects), and a hybrid method based on RANS-LES chained to a FWH integral. The first one seems very promising, providing PSD in a quite good agreement with the measurements. The second, although more advanced, is still challenging, giving reliable OASPL directivities, but unexplained shift in frequency looking to the PSDs. This point is under investigation. Next step will be to apply these methods (both in 3D) to estimate the efficiency of the wavy edge and to compare with the acoustic performances measured during the tests.

REFERENCES

1. L. Enghardt, *The EU FP7 Research Project FLOCON – Objectives and First Results*, Internoise 2010, Lisbon, Portugal, June (2010).
2. M. Gruber, P. Joseph, P. and T. P. Chong, *Experimental Investigation of Airfoil Self Noise and Turbulent Wake Reduction by the Use of Trailing Edge Serrations*, 16th AIAA/CEAS Conference, 2010-3803, Stockholm, Sweden, June (2010).
3. T. P. Chong, P. F. Joseph, P.O.A.L. Davies, *Design and Performances of an Open Jet Wind Tunnel for Aero-Acoustic Measurement*, Applied Acoustics, **70**, pp. 605-614 (2009).
4. R. K. Amiet, *Acoustic radiation from an airfoil in a turbulent stream*, J. Sound Vibration, **41**(4), p. 407–420 (1975).
5. G. Dufour, H. Deniau, J. F. Boussuge, C. Polacsek, S. Moreau, *Affordable Compressible LES of Airfoil-Turbulence Interaction in a Free Jet*, 17th AIAA/CEAS Conference, Portland, USA (2011).
6. K. L. Hansen, R. M. Kelso, B. B. Dally, *Performance Variations of Leading-Edge Tubercles for Distinct Airfoil Profiles*, AIAA Journal, **49**, No. 1, January (2011).
7. D. S. Miklosovic, M. M. Murray, L. E. Howle and F. E. Fish, *Leading-edge Tubercles Delay Stall on Humpback Whale (Megaptera novaeangliae) Flippers*, Physics of Fluids, **16**, No. 5, May (2004).
8. S. Redonnet, E. Manoha, P. Sagaut, *Numerical Simulation of Propagation of Small Perturbations Interacting with Flows and Solid Bodies*, 7th AIAA/CEAS Conference, 2001-222 (2001).
9. G. Reboul, C. Polacsek, *Towards Numerical Simulation of Fan Broadband Noise Aft Radiation From Aero-engines*, AIAA Journal, **48**, Issue 9, pp. 2038-2048 (2010).
10. J. Casper, F. Farassat, *A new time domain formulation for broadband noise predictions*, International Journal of Aeroacoustics, **1**(3), p. 207–240 (2002).
11. M. Dieste, G. Gabard, *Synthetic Turbulence Applied to Broadband Interaction Noise*, 15th AIAA/CEAS Conference , 2009-3267 (2009).
12. C. K. W Tam, Z. Dong, *Radiation and Outflow Boundary Conditions for Direct Computation of Acoustic and Flow Disturbances in a Nonuniform Mean Flow*, J. Computational Acoustics, **4**(2), p. 175-201 (1996).
13. R. Ewert, C. Appel, J. Dierke, M. Herr, *RANS/CAA Based Prediction of NACA 0012 Broadband Trailing Edge Noise and Experimental Validation*, 15th AIAA/CEAS Conference, 2009-3269 (2009).
14. C. Kato, A. Lida, Y. Takamo, H. Fujita, and M. Ikegawa, *Numerical Prediction of Aerodynamic Noise Radiated From Low Mach Number Turbulent Wake*, 31st ASME, AIAA-93-145 (1999).